

# Modulation Format Identification Based on Received Signal Power Distributions for Digital Coherent Receivers

Jie Liu<sup>1</sup>, Zhenhua Dong<sup>2</sup>, Kangping Zhong<sup>1</sup>, Alan Pak Tao Lau<sup>2</sup>, Chao Lu<sup>1</sup> and Yanzhao Lu<sup>3</sup>

<sup>1</sup>Photonics Research Centre, Department of Electronic and Information Engineering, The Hong Kong Polytechnic University, Hung Hom, Kowloon, Hong Kong

<sup>2</sup>Photonics Research Centre, Department of Electrical Engineering, The Hong Kong Polytechnic University, Hung Hom, Kowloon, Hong Kong

<sup>3</sup>Network Research Department, Huawei Technologies, Shenzhen, China

Email: jennyliu@polyu.edu.hk

**Abstract:** We propose a modulation format identification technique based on extracting and identifying specific features of received signal power distributions for digital coherent receivers. Simulation and experimental results demonstrate successful identification among six common modulation formats.

**OCIS codes:** (060.2330) Fiber Optics Communications; (060.1660) Coherent Communications

## 1. Introduction

Elastic Optical Networks (EON) [1] and cognitive optical networks (CON) [2] have recently attracted a lot of interest as future optical networks are envisioned to be more flexible, programmable and efficient in order to support emerging data center and cloud computing applications. As lightpath provisioning will become much more dynamic and incorporate more decision parameters such as Quality of Transmission (QoT) and flexible modulation formats, it may become necessary for a digital coherent receiver to identify the modulation format of incoming signals at the physical layer on-the-fly. Modulation Format Identification (MFI) for wireless systems is an important component for software-defined radio (SDR) and military applications [3]. In optical communication systems however, phase noise effects are more dominant and corresponding frequency offset estimation (FOE) and carrier phase estimation (CPE) techniques are somewhat dependent on modulation format in the first place. A handful of MFI for optical transmissions were recently proposed in the literature but they require very complex iterative algorithms such as  $K$ -means clustering [4], artificial neural networks [5] or Expectation-Maximization (EM) [6].

In this paper, we study received signals after CD compensation and Constant Modulus Algorithm (CMA) for pre-convergence and propose a simple MFI technique based on extracting and identifying specific features from signal power distributions. Simulation results demonstrate successful MFI among QPSK, 16-QAM, 32-QAM, 64-QAM, 128-QAM and 256-QAM signals in practical system OSNRs. Experimental verifications for QPSK/16-QAM identification also show that the proposed MFI technique is tolerant to fiber nonlinearities.

## 2. Operating Principle

Fig. 1 shows the normalized power distributions of six common modulation formats including QPSK, 16-QAM, 32-QAM, 64-QAM, 128-QAM and 256-QAM. In a practical setting, the distribution can be obtained empirically from a block of received symbols  $S$ . Clearly, different modulation formats give rise to different power distributions with distinctive features. For example, the distribution for QPSK is concentrated at 1 while some 64-QAM and 256-QAM

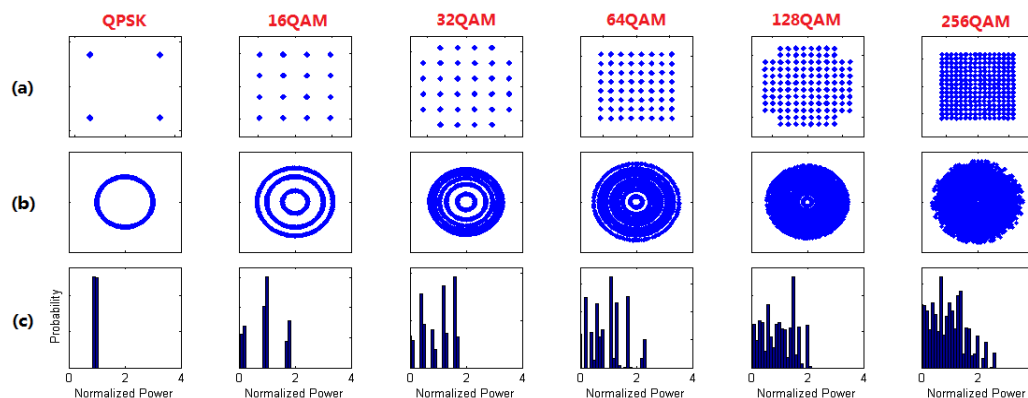


Fig. 1. (a) Constellations; (b) Normalized received signal distributions in presence of frequency offset and other phase impairments; (c) empirical probability distributions of received signal powers for various modulation formats.

Table I. Features of different modulation formats at high OSNR

	QPSK	16QAM	32QAM	64QAM	128QAM	256QAM
Ratio $R_1$ : $P(0.6 \leq S \leq 1.4)/P(S < 0.6 \text{ or } S > 1.4)$	$\infty$	1	<1	<1	<1	<1
Ratio $R_2$ : $P(2.1 \leq S)/P(1.0 \leq S < 1.1)$		0	0	$\infty$	0	0.7
Ratio $R_3$ : $P(0.4 \leq S \leq 0.8)/P(S < 0.4 \text{ or } 0.8 < S \leq 1.2)$		0	1		0.5	0.55
Ratio $R_4$ : $P(2.3 \leq S)/P(2.0 \leq S < 2.3)$					0	1

symbols have noticeably higher power than others in their constellation. Based on these insights, one can extract such distinctive features from the distributions and derive appropriate decision rules for format identification. We propose to use ratios of probability of  $S$  falling on different ranges as such decision metrics. The four ratios  $R_1, R_2, R_3$  and  $R_4$  are detailed in Table I and the corresponding numerical thresholds and decision flow charts for format identification are shown in Fig. 2(a). However, it should be noted that the power distributions and hence the ratios are dependent on OSNR. An example is shown in Fig. 3(a) in which  $R_1$  generally varies with OSNR for both QPSK and 16-QAM signals. Consequently, optimum threshold designs for MFI generally need to take OSNR considerations into account. Rather than a full analytical derivation on the optimal thresholds for all OSNR values, we numerically choose the thresholds for  $R_1, R_2, R_3$  and  $R_4$  that ensure good MFI performance for practical OSNR ranges.

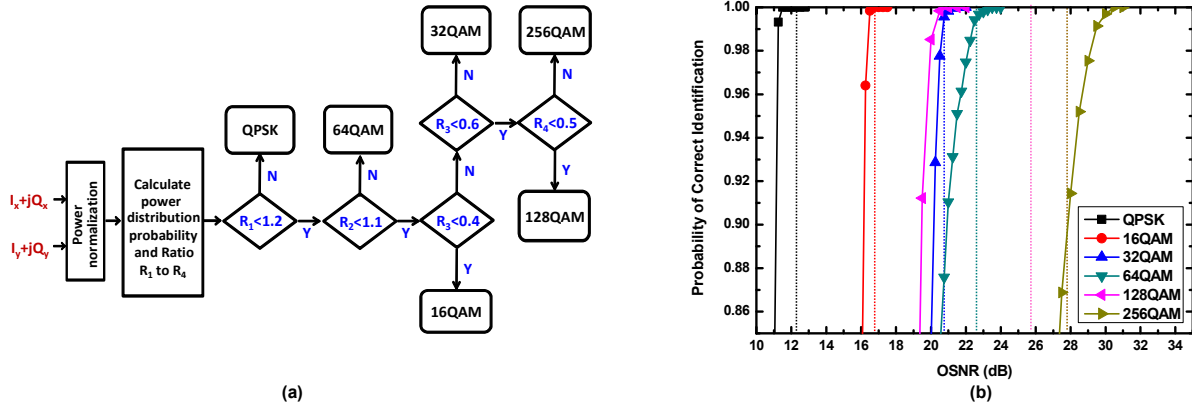


Fig. 2. (a) Decision flow chart for MFI based on received signal power distributions; (b) Probability of correct identification vs. OSNR for various modulation formats. The dotted lines denote forward error correction (FEC) thresholds corresponding to each modulation format.

For each OSNR value, we conduct 5000 independent simulations of polarization-multiplexed (PM) 28Gbaud QPSK, 32Gbaud 16-QAM, 32Gbaud 32-QAM, 32Gbaud 64QAM, 32Gbaud 128-QAM, and 32Gbaud 256-QAM transmissions. 10000 symbols are used to form empirical distributions of received signal power for MFI. With the decision flow chart described in Fig. 2(a), the probabilities of correct format identification for different OSNR values are shown in Fig. 2(b). For each modulation format, the OSNRs that corresponds to forward error correction(FEC) thresholds are also shown as dotted lines for reference (the thresholds are based on BER =  $2e-3$  for QPSK and BER =  $2.4e-2$  for QAM signals). It can be seen that except for 256-QAM signals, virtually 100% correct identification is achieved for all modulation formats when their OSNRs exceed their respective FEC thresholds, indicating that the proposed MFI technique will properly function in practical system settings.

### 3. Experimental Demonstrations

We have also experimentally investigated the proposed MFI technique in distinguishing 112 Gb/s PM-QPSK from 112 Gb/s PM-16QAM signals. The experimental setup is shown in Fig. 3. At the transmitter side, an external cavity laser (ECL) at 1550.12nm is modulated with an I/Q modulator driven by 2-level or 4-level electrical signals to generate the 28Gbaud QPSK or 14Gbaud 16-QAM signals, respectively. The modulated optical signal is polarization multiplexed through polarization beam splitter (PBS), optical delay lines, polarization beam combiner (PBC), amplified and launched into a fiber re-circulating loop. The loop consists of a span of 80 km SSMF, an erbium-doped fiber amplifier (EDFA), an attenuator for OSNR adjustment and a 5nm optical band-pass filter (BPF) for channel power equalization. After transmitting over the fiber loop, the received signal is filtered by a 3<sup>rd</sup> order Gaussian optical BPF with 0.4 nm bandwidth located before an integrated coherent receiver. The linewidth of transmitter and local oscillator (LO) are 150 kHz and 100 kHz respectively and the frequency offset is set to be 1

GHz. The coherently detected signal is sampled by a 50G samples/s real-time oscilloscope and then processed offline. In our experiments, 10000 symbols are used to generate the received power distribution for MFI and the offline DSP include normalization, re-sampling, CD compensation and CMA for polarization de-multiplexing and PMD compensation with step size of  $1e-4$  regardless of modulation format.

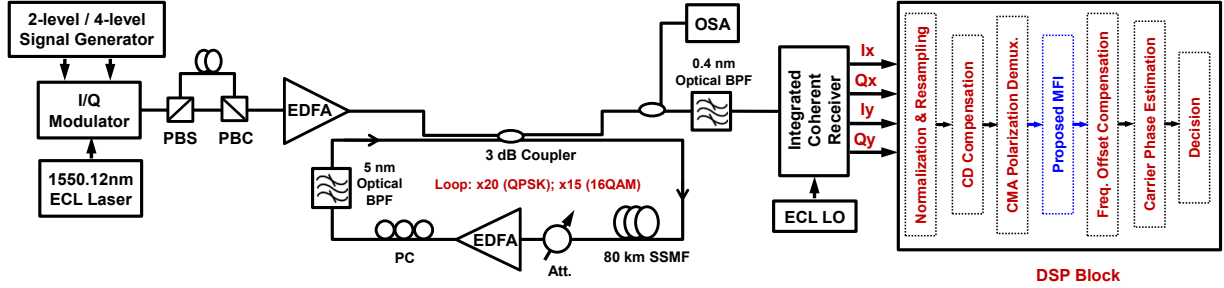


Fig. 3. Experimental setup for modulation format identification. Att: attenuator, PC: polarization controller, BPF: band pass filter.

Fig 4 depicts the MFI performance both for back-to-back and 1600(1200) km transmission of PM-QPSK(16-QAM) signals. Theoretical results assuming circularly symmetric Gaussian ASE noise are also shown for comparison. As shown in Fig. 4(a), with OSNR no less than 12 dB, the 112Gb/s QPSK signal can be successfully distinguished from 112Gb/s 16-QAM signal when the threshold of ratio  $R_I$  is set to 1.2. With 1200 km and 1600 km of transmission, Fig. 4(b) shows that fiber nonlinearity does affect the received power distributions and hence the ratio  $R_I$ , especially for QPSK signals. Nonetheless, for realistic signal launched powers (that gives a BER smaller than the FEC threshold) and even as high as 4 dBm launched power, the same threshold can properly distinguish QPSK from 16-QAM signals.

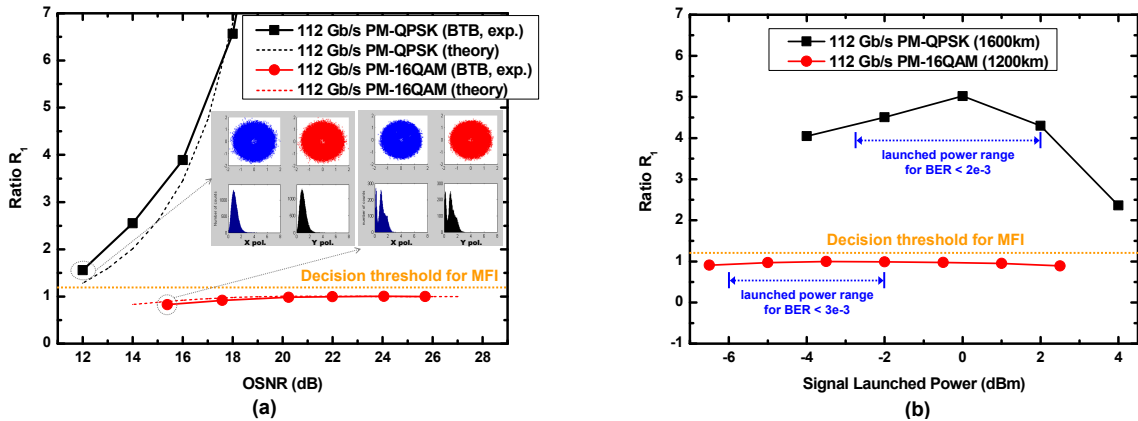


Fig. 4. (a) Ratio  $R_I$  vs. OSNR for back-to-back (inset: normalized received signals after CMA as well as their power distributions) (b) Ratio  $R_I$  vs. signal launched power for 1600 km (PM-QPSK) and 1200 km (PM-16-QAM) transmissions.

#### 4. Conclusions

We proposed and demonstrated a simple MFI technique based on identifying distinctive features extracted from the distributions of the received signal power. The proposed method requires fairly simple DSP and is insensitive to phase impairments. Successful MPI was realized among QPSK, 16-QAM, 32-QAM, 64-QAM, 128-QAM and 256-QAM signals in numerical simulation as well as QPSK and 16QAM signals for experimental data in practical OSNR ranges of interests. The proposed MFI technique can be used for future flexible transmissions requiring dynamic and fast lightpath provisioning.

#### References

- [1] O. Gerstel, M. Jinno, A. Lord, and S. J. Yoo, *IEEE Communication Magazine*, **50**(2), s12-s20 (2012).
- [2] W. Wei, C. Wang, and J. Yu, *IEEE Communications Magazine* **50**, 106-113 (2012).
- [3] O. A. Dobre et al., *IET Commun.*, **1**, 137- 156 (2007).
- [4] N. Guerrero Gonzalez et al., paper no. P6.11, in Proc. ECOC'10, (2010).
- [5] F. N. Khan et al., *Opt. Express* **20**, 12422- 12431 (2012).
- [6] R. Borkowski et al., paper no. OTh3B.3, in Proc. OFC'13, (2013).